Abnormal Structural Networks Characterize Major Depressive Disorder: A Connectome Analysis

Mayuresh S. Korgaonkar, Alex Fornito, Leanne M. Williams, and Stuart M. Grieve

Background: Major depressive disorder (MDD) has been shown to be associated with a disrupted topological organization of functional brain networks. However, little is known regarding whether these changes have a structural basis. Diffusion tensor imaging (DTI) enables comprehensive whole-brain mapping of the white matter tracts that link regions distributed throughout the entire brain, the so-called human connectome.

Methods: We examined whole-brain structural networks in a cohort of 95 MDD outpatients and 102 matched control subjects. Structural networks were represented by an 84 × 84 connectivity matrix representing probabilistic white matter connections between 84 parcellated cortical and subcortical regions using DTI tractography. Network-based statistics were used to assess differences in the interregional connectivity matrix between the two groups, and graph theory was used to examine overall topological organization.

Results: Our network-based statistics analysis demonstrates lowered structural connectivity within two distinct brain networks that are present in depression: the first primarily involves the regions of the default mode network and the second comprises the frontal cortex, thalamus, and caudate regions that are central in emotional and cognitive processing. These two altered networks were observed in the context of an overall preservation of topology as reflected as no significant group differences for the graph-theory measures.

Conclusions: This is the first report to use DTI to show the structural connectomic alterations present in MDD. Our findings highlight that altered structural connectivity between nodes of the default mode network and the frontal-thalamo-caudate regions are core neurobiological features associated with MDD.

Key Words: Biomarker, connectome, diffusion tensor imaging, graph theory, major depressive disorder, network based statistics

Depression is increasingly being conceptualized as a disorder that results from abnormal interactions between brain regions that regulate both emotional and cognitive functions (1,2). These abnormalities primarily involve frontal-limbic regions that include the dorsolateral prefrontal cortex (DLPFC), the anterior cingulate cortex (ACC), and the amygdala-hippocampal complex (3–5). Recent evidence also indicates an important role for an additional circuit, the default mode network (DMN). This is a network of regions associated with the brain's self-referential activity during rest, which normally gets down-regulated during goal-directed tasks to allow more effective focusing (6,7). The prolonged self-referential emotional states that underlie depression may fail to effectively attenuate this network, thereby interfering with normal cognitive and executive functions. Both of these models have been supported by a number of studies that used neuroimaging to evaluate the anatomical components of these systems (8).

Although this reductionist approach of segregating the brain based on existing theories has been valuable in identifying the neurobiological basis that underlies depression, it provides a limited window into a whole systems-level understanding of the abnormalities present in depression (9). In contrast, connectomics is an emerging field that conceptualizes the whole brain as an interconnected network. Advances in the neuroimaging techniques of resting state functional magnetic resonance imaging (rs-fMRI) and diffusion tensor imaging (DTI) have enabled the mapping of the high-resolution functional and structural networks through which the brain is interconnected, the so-called functional and structural human connectome (10).

Recent advances in network-based statistic (NBS) analysis and graph theory have made it possible to analyze the enormous dataset that the human connectome represents in a way that is both tractable and intuitive (11). Graph theory permits the calculation of summary measures of connectivity that can help contextualize the diffuse alterations that may occur across the brain or alterations that may either underlie the key organizational principles of a normal brain or the key organizational abnormalities that characterize a disorder (11,12). Network-based statistics offers a powerful and complementary approach that can be used to characterize the specific features within a network. The use of NBS enables multiple hypothesis testing at a network level, controlling the family-wise error when performing these analyses (e.g., a connectome defined using N nodes or $N \times N$ matrix results in 2^N connections for comparisons) (13).

The methodological advances described above have been utilized by a number of studies that have started conceptualizing mental disorders in terms of abnormalities in whole-brain structural and functional networks (14). Graph theoretic studies of topological properties of brain functional networks in patients with depression have reported an abnormally low average path length—the mean number of connections required to link any

From the The Brain Dynamics Centre (MSK, LMW, SMG), Sydney Medical School-Westmead and Westmead Millennium Institute for Medical Research; and Discipline of Psychiatry (MSK), University of Sydney Medical School: Western, Westmead Hospital, Sydney; and Monash Clinical and Imaging Neuroscience (AF), School of Psychology and Psychiatry & Monash Biomedical Imaging, Monash University, Clayton, Victoria, Australia; Department of Psychiatry and Behavioral Sciences (LMW), Stanford University, Stanford, California; and Sydney Translational Imaging Laboratory (SMG), Sydney Medical School, University of Sydney; Department of Radiology (SMG), Royal Prince Alfred Hospital; and Charles Perkins Centre (SMG), University of Sydney, Camperdown, Australia.

Address correspondence to Stuart M. Grieve, Ph.D., University of Sydney, Sydney Medical School, The Brain Dynamics Center, 36 Larkin St, Waverton, NSW 2060, Australia; E-mail: sgrieve@med.usyd.edu.au.

Received Dec 10, 2013; revised Feb 12, 2014; accepted Feb 13, 2014.

0006-3223/$36.00
http://dx.doi.org/10.1016/j.biopsych.2014.02.018

given pair of nodes in the network—and higher global efficiency (which is inversely related to path length). This has been interpreted as a subtle randomization of network connectivity (15). The same study also found increased betweenness centrality—an index of how central a region is on the shortest paths linking different regions—for areas comprising the DMN. An independent study found a significant reorganization of regional connectivity in major depressive disorder (MDD), though the same set of topological differences was not replicated (16). Similarly, a study of patients with late-life depression did not detect group differences in topological network measures, but there was some evidence to support an overall increased connectivity and changes in average distance between connected nodes (17). These findings point to a diverse set of higher order functional connectivity changes in MDD. An important question is whether these changes have a structural basis. Preliminary work using interregional co-variations in gray matter volume as an indirect measure of structural connectivity found evidence for weaker regional connectivity in MDD patients, coupled with lower clustering and longer path lengths across the network (18). This is supported by data from two studies that reported altered global (increased mean path length and reduced network connectivity strength and global efficiency) and nodal characteristics (in cognitive-emotional and frontoparietal circuitry) in white matter topological networks using DTI (19,20). Two previous studies have used whole-brain DTI to discriminate participants with MDD from participants without MDD (21,22); however, no previous study has used DTI and network-based statistics to map the characteristic network alterations of structural connectivity in a nongeriatric MDD cohort.

The goal of the present study was to map the structural connectomic changes present in MDD using DTI. We examined a highly powered sample, which represents the largest single-site study of structural imaging in depression. We hypothesized that if DMN abnormalities represent the most important feature of pathophysiological alterations in MDD, then disruptions of connectivity to putative DMN nodes—including the rostral ACC (rACC), posterior cingulate cortex (PCC), and precuneus—should be more prominent. Alternatively, if dysfunction of mood-regulation systems is core, then altered connectivity of prefrontal, medial temporal, and limbic structures should be most severe. A final possibility was that our whole-brain analysis would identify hitherto unidentified systems relevant to understanding brain network disruptions in MDD. We first employed an unbiased connectome-wide approach using a recently developed technique (13) to map group differences in the microstructure of each and every connection linking 84 regions distributed throughout the brain. We then used graph theory to evaluate higher order changes in brain network organization.

Methods and Materials

Participant Characteristics and Study Protocol

The iSPOT-D study protocol, clinical assessments, inclusion/exclusion criteria, and diagnosis procedures have been previously described (23,24). In short, the Mini-International Neuropsychiatric Interview, according to DSM-IV criteria, and a 17-item Hamilton Rating Scale for Depression score $\geq$16 confirmed the primary diagnosis of MDD. All MDD participants were either antidepressant medication naïve or had undergone a washout period of at least five half-lives of a previously prescribed antidepressant medication. Baseline magnetic resonance imaging (MRI) data were available from the first 102 MDD participants and 102 age- and gender-matched healthy participants. Diffusion tensor imaging data for seven participants were not collected at baseline, resulting in 95 MDD participants suitable for analysis. This study was approved by the Western Sydney Ethics Committee; participants provided written informed consent.

Image Acquisition

Magnetic resonance imaging utilized a 3.0T General Electric (Milwaukee, Wisconsin) Signa HDx scanner with an 8-channel head coil. T1-weighted three-dimensional (3-D) spoiled gradient recalled parameters included 180 sagittal 1 mm slices; 1 mm isotropic; 256 $\times$ 256 matrix; repetition time = 8.3 msec; echo time = 3.2 msec; flip angle = 11°; and inversion time = 500 msec. Diffusion tensor imaging parameters included 70 axial contiguous 2.5 mm slices; 1.72 mm $\times$ 1.72 mm resolution; 128 $\times$ 128 matrix; repetition time = 17,000 msec; echo time = 95 msec; frequency direction = right/left; 42 diffusion orientations; and b-value = 1250.

MRI Cortical Parcellation

We used Freesurfer (v4.3) (http://surfer.nmr.mgh.harvard.edu/) for segmentation of the 3-D T1-weighted structural images, as previously described (25,26). In brief, a two-dimensional cortical surface was calculated and automatically divided into 35 gyral-based anatomically labeled areas for each hemisphere using the Desikan-Killiany atlas (27). An automatic subcortical parcellation was also performed based on probabilistic information of location of subcortical structures automatically estimated from a manually labeled training dataset (28). Cortical segmentation and anatomical labels were validated by manual inspection. All the cortical regions and seven subcortical structures (amygdala, hippocampus, thalamus, caudate, putamen, palladium, and nucleus accumbens) were used in this analysis to generate the connectivity matrix.

DTI Processing

Diffusion tensor imaging data were preprocessed and analyzed using the Oxford Centre for Functional MRI of the Brain Diffusion Toolbox (v4.1.3) (http://www.fmrib.ox.ac.uk/fsl) (22,25). The raw DTI data were corrected for head movement and eddy current distortions. Diffusion tensor models were then fitted independently for each voxel within the brain. The segmented cortical regions for each participant were transformed into DTI space using a 3-D rigid-body six-parameter registration, maximizing mutual information between the nondiffusion-weighted image and T1-weighted anatomical data.

Network Analysis of DTI Data

Figure 1 summarizes the analysis workflow. We analyzed interregional white matter connectivity using a multi-fiber diffusion probabilistic model that estimates probability distributions for one or more fiber populations at each brain voxel (29). These probability distributions guide multiple fiber samples starting from a seed voxel (seed) to a specified target region. Tractography was performed using each of the regional labels as seed and the remaining labels as targets. One thousand sample tracts were generated from each voxel within the seed region, and only tracts that reached the target region were retained. The tracts were terminated once they reached a particular target region. For the 42 brain structures, this resulted in an 84 $\times$ 84 interregional

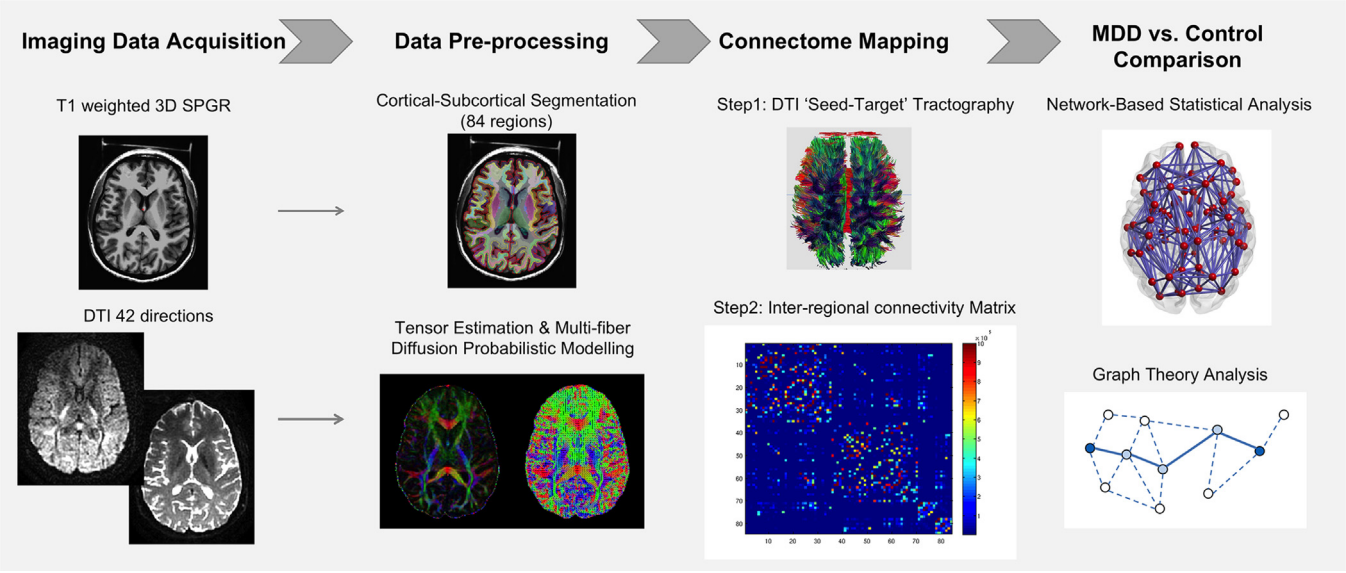

Figure 1. Analysis workflow. 3D, three-dimensional; DTI, diffusion tensor imaging; MDD, major depressive disorder; SPGR, spoiled gradient recalled.

connectivity matrix for each participant. For this matrix, the diagonal elements represent self-connections and are excluded from this analysis. The upper half of the diagonal in this matrix contains connections that are also represented in the lower half. Ideally, these should be symmetric (i.e., the fiber pathway from cortical seed region A to target region B should be equivalent to that from seed region B to target region A). For the purposes of our analysis, the larger of the two values was used to represent the number of probabilistic tracts or fiber pathways that connect the two regions.

NBS Analyses

The NBS analysis method (13) was used to assess differences in the interregional connectivity matrix between the MDD and control groups. Analogous to cluster-based thresholding strategies used in voxel-wise MRI studies, this method deals with the multiple comparisons problem posed by connectomic data (in an undirected network of N regions, there are $N[N-1]/2$ connection values) by evaluating the null hypothesis at the level of interconnected subnetworks rather than individual connections. In this method, identifying subnetworks is similar to identifying significant clusters of activation in traditional functional magnetic resonance imaging studies. We first performed a two-sample t test at each edge independently to test for significant differences in the value of connectivity between the two groups. A primary component-forming threshold ($p < .001$, uncorrected) was then applied to form a set of suprathreshold edges. This identifies all the possible connected components, or subnetworks, in the matrix at this uncorrected level. Next, the size of the remaining connected components—sets of nodes that can be linked by suprathreshold connections—in the network was computed. The statistical significance of the size of each observed component was then evaluated with respect to an empirical null distribution of maximal component sizes obtained under the null hypothesis of random group membership (1000 permutations). Subnetworks that were significant at a corrected level of $p < .05$ were reported. The BrainNet viewer (http://www.nitrc.org/projects/bnv/) was used to visualize the significant subnetworks and to make figures (30).

Graph Theory Analyses

Graph theoretic analyses were performed on the interregional connectivity matrices (weighted undirected networks) using the Brain Connectivity Toolbox (http://www.brain-connectivity-toolbox.net/) (31). To enable comparison of global network properties across participants and groups, we used a sparsity (connection density) threshold (S), which retains S% of the top connections for each participant. This threshold ensured that the number of nodes and connections were matched across participants. To avoid biases associated with using a single threshold, we examined topological properties across a range of thresholds ($10\% < S < 30\%$ in steps of 1%). The range of thresholds was selected based on previous work, which has shown that the networks are small-world within this regime (15). At each of these thresholds, we calculated the following global network measures: 1) the characteristic path length (the mean number of connections on the shortest path between any two regions in the network); 2) the clustering coefficient, which quantifies the probability that two nodes connected to an index node are also connected with each other; and 3) global efficiency, computed as the harmonic mean of the inverse path length. We also examined the following local nodal characteristics of the individual network regions: 1) nodal degree, which is defined as the number of connections a particular node has with the rest of the network; 2) betweenness centrality, which is a measure of the number of shortest paths that traverse a given node and is used to detect highly central network nodes; and 3) local efficiency, which measures the efficiency of the subgraph defined by an index node's neighbors after removal of that node and putatively indexes fault tolerance. For all measures, we computed the area under the curve across the full range of sparsity thresholds for comparison between MDD and control groups. Assessments for the global measures were performed using a $p < .016$ (corrected for number of measures; i.e., .05/3), whereas a $p < .00059$ (corrected for number of nodes; i.e., .05/84 nodes) was used for the local regional measures.

Correlations between Network and Clinical Measures

The relationship between network measures and MDD severity and duration were assessed for the MDD participants, controlling for age and gender. These assessments were performed only for

the network edges (number of tracts) that were identified in the NBS analysis as showing significant group differences and for the global and local graph measures that were significantly different between the MDD and control groups.

Results

Table 1 shows the demographic and clinical characteristics for the participants with MDD and control subjects. No significant differences in age ($p = .984$) or gender ($\chi^2 = .957$) were present between control subjects and MDD participants.

Whole-Brain Mapping of Connectivity Deficits in MDD

The NBS identified two subnetworks that were significantly different between MDD and control participants ($p < .05$, corrected for multiple comparisons; Figure 2). The first network consisted of eight edges connecting seven different regions (corrected $p = .003$). These connections linked the bilateral rACC and posterior portion of the cingulate cortex (isthmus) with both ipsilateral and contralateral connections between these four regions. Bilateral edges also connected the rACC to the right precuneus. Two further edges connected the left cuneus to the right rACC and the left pericalcarine region (Table 2). The second network consisted of five edges linking six nodes (corrected $p = .023$). These edges connected the right and left superior frontal cortex, the right rostral middle frontal to both the right thalamus and right caudate, the right superior frontal to the right caudate, and the left superior frontal to the right medial orbitofrontal cortex (mOFC). Major depressive disorder participants were found to have a reduced number of reconstructed tracts for each of the connections in both of the identified networks (all connections $p < .002$; Table 2).

Graph Theoretical Analysis

None of the topological measures showed significant differences between the MDD and control groups after correcting for multiple comparisons. At an uncorrected threshold, a difference was observed only for the global characteristic path length (MDD > control subjects; $p = .048$). Table S1 in Supplement 1 summarizes the MDD-related changes in regional nodal characteristics that were significant at an uncorrected threshold.

Correlation Connectivity Measures and Clinical Measures

None of the network connections identified in the network-based statistical analysis or the global or local topological metrics were correlated with either MDD severity or duration.

Table 1. Participant Demographic and Clinical Characteristics

Characteristics	Control Subjects ($n = 102$) *n* (%) or Mean ± SD (Range)	MDD ($n = 95$) *n* (%) or Mean ± SD (Range)
Female	49 (48.0%)	46 (48.4%)
Age (Years)	33.9 ± 13.0 (18–62)	33.8 ± 13.1 (19–65)
Years of Education	14.7 ± 3.5 (6–18)	14.2 ± 2.9 (6–18)
HRSD-17 Baseline	–	20.8 ± 3.7 (16–34)
Age of Onset (Years)	–	22.1 ± 12.5 (5–58)
Disease Duration (Years)	–	11.4 ± 11.8 (0–58)
Number of Episodes	–	12.1 ± 21.0 (1–99)
% Melancholic	–	29.5%

HRSD-17, 17-item Hamilton Rating Scale for Depression; MDD, major depressive disorder.

Discussion

This study is the first report on connectome-level differences in structural networks between a depressed and nondepressed group. Our NBS analysis demonstrates that two distinct brain networks characterize the structural connectivity abnormalities that are present in depression. This is a striking finding, as the anatomical regions involved are central to prevailing theories of depression, consistent with our hypothesis (1,2,6). The first of these two networks involves the regions of the DMN, specifically the rACC and isthmus portion of the PCC bilaterally and the right precuneus, in addition to the left cuneus and pericalcarine regions. The second network is comprised of a frontal-subcortical network that involves the bilateral superior frontal and the rostral middle frontal, mOFC, thalamus, and caudate regions in the right hemisphere. These two altered networks were observed in the context of an overall preserved topology, as reflected in our graph theoretical analyses.

The ability to measure the connectome using DTI is a major methodological step forward; however, this complex dataset presents serious analytical challenges. These challenges are largely overcome by graph theoretical analysis and network-based statistics. This study used both graph theoretical and network-based statistical analyses of DTI data in characterizing structural organizational abnormalities in major depression. Our data show two clear subnetworks that differentiate MDD participants from control subjects. In both systems, microstructural measures of connectivity were reduced in MDD participants. The largest of the two significant circuits primarily involved key components of the DMN (32), confirming the centrality of this network in the pathophysiology of MDD. The second network is centered around an axis defined by key frontal and subcortical regions that are central to cognitive and emotion processing and that have all been previously implicated in major depression by neuroimaging studies.

These direct structural connectomic measures complement our recent analysis of gray matter changes in the same cohort, which revealed extensive gray matter volumetric loss affecting these same regions (33). Gray matter volumetric reductions were seen bilaterally in the cortical regions that form part of the abnormal circuits described above (i.e., bilaterally in the rACC and mid to posterior portions of the cingulate gyrus, including the isthmus, precuneus, cuneus, superior-middle frontal gyrus regions mapping the dorsolateral and dorsomedial prefrontal cortex [dmPFC], and the mOFC). The same subcortical regions that showed gray matter loss were also involved in abnormal MDD circuits; however, the laterality was reversed, with lower volume present in the left thalamus and left caudate versus the involvement of the right corresponding region in the MDD circuits. The structural decline in these regions may influence the number of probabilistic tracts that arrive or leave from the regions. To check if the reduced volume could explain the finding of a reduced number of reconstructed tracts for the MDD group, we evaluated the correlation between these measures for the rACC. The number of tracts were not influenced by the gray matter volume for the region ($r < .149$ and $p > .05$ for all the tracts in network 1 related to the rACC). Meta-analyses of functional imaging studies in depression have highlighted the role of the DLPFC, the ACC, and the dmPFC regions in depression (2,34,35). We have previously demonstrated task-based abnormal activations to cognitive and emotional tasks in MDD participants in regions of interest that are contained by the frontal-subcortical network that we isolated in the present study using NBS (36). The rostral

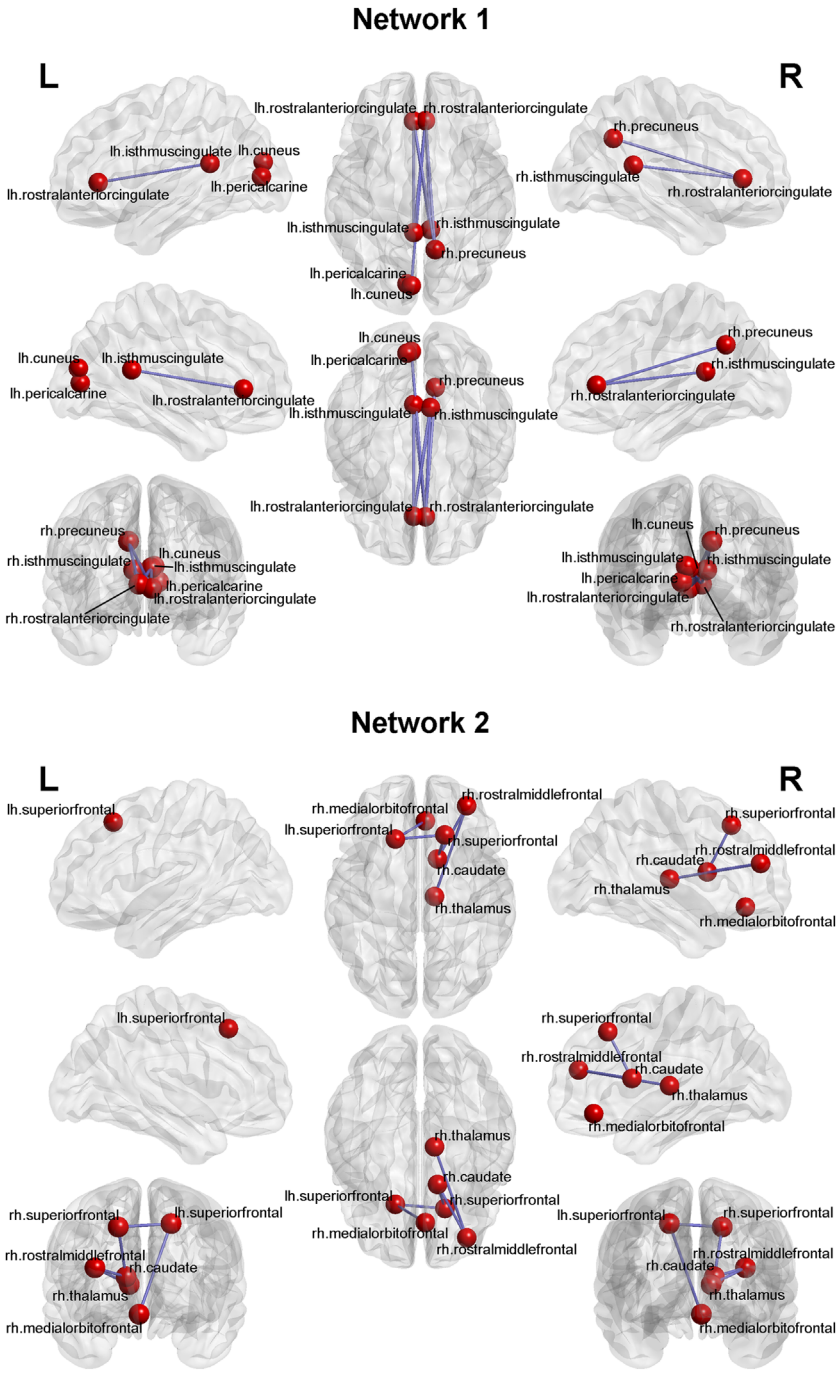

Figure 2. Summary of significant networks that characterize major depressive disorder using network-based statistical analysis. The two distinct circuits are represented. The circuit depicted at the top (Network 1) consists of eight nodes and seven edges and primarily involves regions known to be involved in the default mode network. The circuit depicted at the bottom (Network 2) contains a central cluster of six nodes involving the frontal-subcortical regions: the right thalamus, right caudate, right medial orbitofrontal cortex, right rostral middle frontal, and both the left and right superior frontal cortex. L, left; lh, left hand; R, right; rh, right hand.

middle frontal and thalamic structural connection identified in the second network is consistent with the importance of the functional connection between these regions in treatment-resistant depression (37).

Effective downregulation of the DMN is essential for a range of active cognitive tasks, including those characteristically impaired in depression such as executive function and emotional regulation. A range of evidence implicates the rACC—which includes the subgenual ACC (sgACC)—as a central region in depression, with metabolic, structural, and connectivity data linking severity and prognosis to this region (38). Resting state connectivity of subgenual components of the DMN has been previously shown to be stronger in MDD, a reduction that is coupled with metabolic overactivity in this region and that has been interpreted as driving a disproportionate upregulation of the DMN (39). In keeping with the idea of DMN overactivity as a core feature of MDD, treatments that focus on deep-brain stimulation of the sgACC in treatment-resistant depression cause symptomatic improvement and are also associated with decreased metabolism in this area (40). A recent study has also linked higher rs-fMRI dmPFC-sgACC and sgACC-DLPFC connectivity and lower dmPFC-medial dorsal thalamus, dmPFC-putamen, and sgACC-amygdala/hippocampus functional magnetic resonance imaging connectivity to improved response to repetitive transcranial magnetic

Table 2. Networks Identified to be Significantly Different between the MDD and Control Groups Using Network-Based Statistical Analysis

	Number of Probabilistic Tracts		
	Control ($n = 102$)	MDD ($n = 95$)	
Networks and Connections	(Mean ± SD)	(Mean ± SD)	t and p Value
Network 1			
L-cuneus and L-pericalarine	789222 ± 177512	688755 ± 168292	$t = 4.06$, $p < .001$
L-isthmus cingulate and L-rACC	32765 ± 25999	20335 ± 20455	$t = 3.69$, $p < .001$
L-rACC and R-isthmus cingulate	4985 ± 5519	2648 ± 3472	$t = 3.51$, $p < .001$
L-rACC and R-precuneus	7939 ± 9218	4395 ± 5392	$t = 3.25$, $p = .001$
L-cuneus and R-rACC	419 ± 755	140 ± 359	$t = 3.25$, $p = .001$
L-isthmus cingulate and R-rACC	3205 ± 3738	1440 ± 1653	$t = 4.21$, $p < .001$
R-isthmus cingulate and R-rACC	23982 ± 22272	15356 ± 15043	$t = 3.15$, $p = .002$
R-precuneus and R-rACC	30631 ± 32691	17715 ± 17015	$t = 3.43$, $p = .001$
Network 2			
L-superior frontal and R-medial orbitofrontal	125889 ± 91970	87796 ± 65735	$t = 3.31$, $p = .001$
L-superior frontal and R-superior frontal	2627049 ± 1165053	2026769 ± 991112	$t = 3.87$, $p < .001$
R-rostral middle frontal and R-thalamus	275981 ± 163175	201224 ± 136524	$t = 3.46$, $p = .001$
R-rostral middle frontal and R-caudate	379234 ± 218452	286321 ± 193670	$t = 3.14$, $p = .002$
R-superior frontal and R-caudate	132741 ± 106124	89711 ± 76208	$t = 3.24$, $p = .001$

Mean and standard deviations for the number of probabilistic tracts for the different connections in each of the networks are summarized.
L, left; MDD, major depressive disorder; R, right; rACC, rostral anterior cingulate cortex.

stimulation (41). Our network analysis not only provides the basis for considering rACC/sgACC and DMN dysfunction in a complete whole-brain context but also independently validates the centrality of the structural connections of these same key regions.

Previous connectomic analyses in MDD have measured functional connectivity using rs-fMRI or structural connectivity using gray matter volume. Notably, all of the functional connectomic analyses in MDD have been performed using moderately sized cohorts. These provide a general lack of consensus, making it difficult to generalize from these findings. The results of a more highly powered analysis of structural connectivity by Singh *et al.* (18) are consistent with our data, showing that MDD is characterized by longer average path lengths (although significant at uncorrected level in our study). Longer path lengths have also been seen using DTI in remitted geriatric depression and are consistent with poorer global efficiency (19). Singh *et al.* (18) also found altered nodal connectivity in a range of regions, including the left ACC and left inferior temporal lobe (both decreased) and in the left middle temporal lobe and mOFC (both increased). Despite some of these commonalities, our results do not exactly mirror the networks derived from these volume data. Some of these discrepancies could be attributed to the nature of measures used in the topological analyses; the gray matter volume measures represent covariance between regions, while DTI measures represent a more direct measure of structural connectivity. Though no significant group differences in node-level topological properties were identified at corrected thresholds, some interesting results at uncorrected thresholds were observed: namely, nodal degree was reduced in fronto-limbic-subcortical regions; betweenness centrality was altered in right superior frontal gyrus, a result consistent with a prior report (19); and local efficiency was increased in temporoparietal regions for the MDD group. These findings require replication but highlight the importance of these key hubs within the brain network for depression.

Only one other study has reported an association between graph theoretic measures of network organization and clinical characteristics in depression. Zhang *et al.* (15) found nodal centrality properties of the hippocampus and caudate (calculated using rs-fMRI connectome measures) to be associated with disease duration and severity. However, this association was not replicated with the structural measures used in our study. The lack of correlation between the network measures and the clinical measures suggests that the structural circuits that define diagnosis may not be the abnormalities that result in a more severe expression of depressive symptoms or cause depressive symptoms to persist over time.

This study has several limitations. Although our analysis is highly powered, the results require replication to further establish validity and enable generalization. Any analysis using DTI is subject to inaccuracies relating to the limitations of this technique in resolving crossing fibers and sharp angulations of tracts (42). This can lead to false-positive connections, particularly between the left and right regions on the medial wall, which are located close to each other, as well as false negatives, particularly for long-range tracts. These may substantially distort measures from the graph theoretical approaches. Only anatomical validations can resolve this issue, though there are insufficient human data at present. In recognition of this limitation, we used a probabilistic tractography approach that partially overcomes these limitations (29). Since the same technique was applied identically to both control and MDD groups, these problems should pose no bias in detecting group differences. Due to the potential for diffusion tractography to generate false positives and false negatives in tract reconstruction, the precise positioning of the affected subnetworks should be interpreted with caution. For example, NBS identified differences between the interhemispheric rACC and left PCC/cuneus regions, a tract that has not previously been described in the animal tract tracing literature. As such, our findings provide an estimate of the general location of structural network differences (e.g., anterior-to-posterior cingulate connectivity) and the precise regional pairs linked by a disrupted connection should be interpreted cautiously. This is a limitation common to all DTI studies, and the field will benefit from the development of novel acquisition sequences and tractography algorithms to improve the accuracy of tract reconstruction. Defining a functionally valid parcellation of the brain is an open problem in connectomics, and all available approaches have

strengths and limitations (12,43,44). We used an anatomical parcellation in our analysis to retain consistency with resolutions used in prior reports (15,18,19). Typically, the results obtained with different parcellations of a comparable resolution tend to be consistent (45,46) but may vary when different resolutions are used. A future analysis examining how connectivity changes in MDD vary as a function of template resolution may be useful in identifying whether these abnormalities are only present at certain spatial scales.

In summary, we used network analyses of structural (DTI) connectome data to describe two abnormal structural networks that characterize MDD patients. These networks relate to two key motifs implicated in both resting state and task-based functional data: the default mode network and the frontal-thalamus-caudate regions. Major depressive disorder participants had reduced connectivity in both of these networks. Despite these robust findings, there was no correlation between the identified network connections and either duration or severity of depression. These results provide the first evidence of an anomalous structural connectome in major depression.

We acknowledge Brain Resource Company Operations Pty Ltd as the sponsor for the iSPOT-D study (NCT00693849). SMG acknowledges the support of the Sydney University Medical Foundation.

We thank Claire Day and Catherine King (Global Study Coordinators), as well as the iSPOT-D Publication Team, for their valuable input into this manuscript and into the study overall. We gratefully acknowledge the editorial support of Jon Kilner, MS, MA (Pittsburgh, Pennsylvania). We thank Dr. Lavier Gomes, Ms. Sheryl Foster, and the Department of Radiology at Westmead Hospital for their substantial contributions to magnetic resonance imaging data acquisition.

Dr. Grieve has received fees as a consultant from Brain Resource. Dr. Williams has received consultant fees from Brain Resource and was a stockholder in Brain Resource. Dr. Korgaonkar and Dr. Fornito report no biomedical financial interests or potential conflicts of interest.

ClinicalTrials.gov: International Study to Predict Optimized Treatment - in Depression (iSPOT-D); http://www.clinicaltrials.gov/ct2/show/NCT00693849?term=iSPOT-D&rank=1; NCT00693849.

Supplementary material cited in this article is available online at http://dx.doi.org/10.1016/j.biopsych.2014.02.018.

1. Drevets WC (2007): Orbitofrontal cortex function and structure in depression. *Ann N Y Acad Sci* 1121:499–527.
2. Hamilton J, Etkin A (2012): Functional neuroimaging of major depressive disorder: A meta-analysis and new integration of baseline activation and neural response data. *Am J Psychiatry* 169:693–704.
3. Drevets WC, Price JL, Furey ML (2008): Brain structural and functional abnormalities in mood disorders: Implications for neurocircuitry models of depression. *Brain Struct Funct* 213:93–118.
4. Gotlib IH, Hamilton JP (2008): Neuroimaging and depression: Current status and unresolved issues. *Curr Dir Psychol Sci* 17:159–163.
5. Mayberg HS (2003): Modulating dysfunctional limbic-cortical circuits in depression: Towards development of brain-based algorithms for diagnosis and optimised treatment. *Br Med Bull* 65:193–207.
6. Northoff G, Wiebking C, Feinberg T, Panksepp J (2011): The 'resting-state hypothesis' of major depressive disorder-a translational subcortical-cortical framework for a system disorder. *Neurosci Biobehav Rev* 35:1929–1945.
7. Sheline YI, Barch DM, Price JL, Rundle MM, Vaishnavi SN, Snyder AZ, *et al.* (2009): The default mode network and self-referential processes in depression. *Proc Natl Acad Sci U S A* 106:1942–1947.
8. Korgaonkar MS, Grieve SM, Koslow SH, Gabrieli JD, Gordon E, Williams LM (2011): Loss of white matter integrity in major depressive disorder: Evidence using tract-based spatial statistical analysis of diffusion tensor imaging. *Hum Brain Mapp* 32:2161–2171.
9. Behrens TE, Sporns O (2012): Human connectomics. *Curr Opin Neurobiol* 22:144–153.
10. Hagmann P, Cammoun L, Gigandet X, Meuli R, Honey CJ, Wedeen VJ, Sporns O (2008): Mapping the structural core of human cerebral cortex. *PLoS Biol* 6:e159.
11. Bullmore E, Sporns O (2009): Complex brain networks: Graph theoretical analysis of structural and functional systems. *Nat Rev Neurosci* 10:186–198.
12. Fornito A, Zalesky A, Breakspear M (2013): Graph analysis of the human connectome: Promise, progress, and pitfalls. *Neuroimage* 80: 426–444.
13. Zalesky A, Fornito A, Bullmore ET (2010): Network-based statistic: Identifying differences in brain networks. *Neuroimage* 53:1197–1207.
14. Fornito A, Bullmore ET (2012): Connectomic intermediate phenotypes for psychiatric disorders. *Front Psychiatry* 3:32.
15. Zhang J, Wang J, Wu Q, Kuang W, Huang X, He Y, Gong Q (2011): Disrupted brain connectivity networks in drug-naive, first-episode major depressive disorder. *Biol Psychiatry* 70:334–342.
16. Lord A, Horn D, Breakspear M, Walter M (2012): Changes in community structure of resting state functional connectivity in unipolar depression. *PloS One* 7:e41282.
17. Bohr IJ, Kenny E, Blamire A, O'Brien JT, Thomas AJ, Richardson J, Kaiser M (2013): Resting-state functional connectivity in late-life depression: Higher global connectivity and more long distance connections. *Front Psychiatry* 3:116.
18. Singh MK, Kesler SR, Hadi Hosseini SM, Kelley RG, Amatya D, Hamilton JP, *et al.* (2013): Anomalous gray matter structural networks in major depressive disorder. *Biol Psychiatry* 74:777–785.
19. Bai F, Shu N, Yuan Y, Shi Y, Yu H, Wu D, *et al.* (2012): Topologically convergent and divergent structural connectivity patterns between patients with remitted geriatric depression and amnestic mild cognitive impairment. *J Neurosci* 32:4307–4318.
20. Qin J, Wei M, Liu H, Yan R, Luo G, Yao Z, Lu Q (2013): Abnormal brain anatomical topological organization of the cognitive-emotional and the frontoparietal circuitry in major depressive disorder [published online ahead of print November 22]. *Magn Reson Med.* doi:10.1002/mrm.25036.
21. Fang P, Zeng L-L, Shen H, Wang L, Li B, Liu L, Hu D (2012): Increased cortical-limbic anatomical network connectivity in major depression revealed by diffusion tensor imaging. *PloS One* 7:e45972.
22. Korgaonkar MS, Cooper NJ, Williams LM, Grieve SM (2012): Mapping inter-regional connectivity of the entire cortex to characterize major depressive disorder: A whole-brain diffusion tensor imaging tractography study. *Neuroreport* 23:566–571.
23. Grieve SM, Korgaonkar MS, Etkin A, Harris A, Koslow SH, Wisniewski S, *et al.* (2013): Brain imaging predictors and the international study to predict optimized treatment for depression: Study protocol for a randomized controlled trial. *Trials* 14:224.
24. Williams LM, Rush AJ, Koslow SH, Wisniewski SR, Cooper NJ, Nemeroff CB, *et al.* (2011): International Study to Predict Optimized Treatment for Depression (iSPOT-D), a randomized clinical trial: Rationale and protocol. *Trials* 12:4.
25. Dale AM, Fischl B, Sereno MI (1999): Cortical surface-based analysis. I. Segmentation and surface reconstruction. *Neuroimage* 9:179–194.
26. Grieve SM, Korgaonkar MS, Clark CR, Williams LM (2011): Regional heterogeneity in limbic maturational changes: Evidence from integrating cortical thickness, volumetric and diffusion tensor imaging measures. *Neuroimage* 55:868–879.
27. Desikan RS, Segonne F, Fischl B, Quinn BT, Dickerson BC, Blacker D, *et al.* (2006): An automated labeling system for subdividing the human cerebral cortex on MRI scans into gyral based regions of interest. *Neuroimage* 31:968–980.
28. Fischl B, Salat DH, Busa E, Albert M, Dieterich M, Haselgrove C, *et al.* (2002): Whole brain segmentation: Automated labeling of neuroanatomical structures in the human brain. *Neuron* 33:341–355.
29. Behrens TE, Berg HJ, Jbabdi S, Rushworth MF, Woolrich MW (2007): Probabilistic diffusion tractography with multiple fibre orientations: What can we gain? *Neuroimage* 34:144–155.
30. Xia M, Wang J, He Y (2013): BrainNet Viewer: A network visualization tool for human brain connectomics. *PLoS One* 8:e68910.

31. Rubinov M, Sporns O (2010): Complex network measures of brain connectivity: Uses and interpretations. *Neuroimage* 52:1059–1069.
32. Greicius MD, Krasnow B, Reiss AL, Menon V (2003): Functional connectivity in the resting brain: A network analysis of the default mode hypothesis. *Proc Natl Acad Sci U S A* 100:253–258.
33. Grieve SM, Korgaonkar MS, Koslow SH, Gordon E, Williams LM (2013): Widespread reductions in grey matter volume in depression. *Neuroimage Clin* 3:332–339.
34. Fitzgerald PB, Oxley TJ, Laird AR, Kulkarni J, Egan GF, Daskalakis ZJ (2006): An analysis of functional neuroimaging studies of dorsolateral prefrontal cortical activity in depression. *Psychiatry Res* 148:33–45.
35. Koenigs M, Grafman J (2009): The functional neuroanatomy of depression: Distinct roles for ventromedial and dorsolateral prefrontal cortex. *Behav Brain Res* 201:239–243.
36. Korgaonkar MS, Grieve SM, Etkin A, Koslow SH, Williams LM (2013): Using standardized fMRI protocols to identify patterns of prefrontal circuit dysregulation that are common and specific to cognitive and emotional tasks in major depressive disorder: First wave results from the iSPOT-D study. *Neuropsychopharmacology* 38:863–871.
37. Li CT, Chen LF, Tu PC, Wang SJ, Chen MH, Su TP, Hsieh JC (2013): Impaired prefronto-thalamic functional connectivity as a key feature of treatment-resistant depression: A combined MEG, PET and rTMS study. *PloS One* 8:e70089.
38. Drevets WC, Savitz J, Trimble M (2008): The subgenual anterior cingulate cortex in mood disorders. *CNS Spectr* 13:663–681.
39. Greicius MD, Flores BH, Menon V, Glover GH, Solvason HB, Kenna H, *et al.* (2007): Resting-state functional connectivity in major depression: Abnormally increased contributions from subgenual cingulate cortex and thalamus. *Biol Psychiatry* 62:429–437.
40. Lozano AM, Mayberg HS, Giacobbe P, Hamani C, Craddock RC, Kennedy SH (2008): Subcallosal cingulate gyrus deep brain stimulation for treatment-resistant depression. *Biol Psychiatry* 64:461–467.
41. Salomons TV, Dunlop K, Kennedy SH, Flint A, Geraci J, Giacobbe P, Downar J (2014): Resting-state cortico-thalamic-striatal connectivity predicts response to dorsomedial prefrontal rTMS in major depressive disorder. *Neuropsychopharmacology* 39:488–498.
42. Wedeen VJ, Wang RP, Schmahmann JD, Benner T, Tseng WY, Dai G, *et al.* (2008): Diffusion spectrum magnetic resonance imaging (DSI) tractography of crossing fibers. *Neuroimage* 41:1267–1277.
43. de Reus MA, van den Heuvel MP (2013): The parcellation-based connectome: Limitations and extensions. *Neuroimage* 80: 397–404.
44. Wig GS, Schlaggar BL, Petersen SE (2011): Concepts and principles in the analysis of brain networks. *Ann N Y Acad Sci* 1224:126–146.
45. Zalesky A, Fornito A, Harding IH, Cocchi L, Yucel M, Pantelis C, Bullmore ET (2010): Whole-brain anatomical networks: Does the choice of nodes matter? *Neuroimage* 50:970–983.
46. Fornito A, Zalesky A, Bullmore ET (2010): Network scaling effects in graph analytic studies of human resting-state FMRI data. *Front Syst Neurosci* 4:22.